

NASA/TM—1999-209075

AIAA-99-0456



Preliminary Evaluation of a 10 kW Hall Thruster

Robert S. Jankovsky
Glenn Research Center, Cleveland, Ohio

Chris McLean and John McVey
Space Power, Inc., San Jose, California

Prepared for the
37th Aerospace Sciences Meeting & Exhibit
sponsored by the American Institute of Aeronautics and Astronautics
Reno, Nevada, January 11-14, 1999

National Aeronautics and
Space Administration

Glenn Research Center

April 1999

Acknowledgments

The authors would like to gratefully acknowledge the support of Mary Kriebel of TRW Inc.

Available from

NASA Center for Aerospace Information
800 Elkridge Landing Road
Linthicum Heights, MD 21090-2934
Price Code: A03

National Technical Information Service
5287 Port Royal Road
Springfield, VA 22100
Price Code: A03

PRELIMINARY EVALUATION OF A 10 kW HALL THRUSTER

Robert S. Jankovsky
NASA Glenn Research Center
Cleveland, Ohio 44135

Chris McLean
John McVey
Space Power, Inc.
San Jose, CA 95134

Abstract

A 10 kW Hall thruster was characterized over a range of discharge voltages from 300-500 V and a range of discharge currents from 15-23 A. This corresponds to power levels from a low of 4.6 kW to a high of 10.7 kW. Over this range of discharge powers, thrust varied from 278 mN to 524 mN, specific impulse ranged from 1644 to 2392 seconds, and efficiency peaked at approximately 59%. A continuous 40 hour test was also undertaken in an attempt to gain insight with regard to long term operation of the engine. For this portion of the testing the thruster was operated at a discharge voltage of 500 V and a discharge current of 20 A. Steady-state temperatures were achieved after 3-5 hrs and very little variation in performance was detected.

Introduction

Beginning in 1990, NASA initiated an effort to evaluate Hall thrusters due to their unique combination of relatively high specific impulse and favorable thrust density. These efforts focused on the state-of-the-art Russian Stationary Plasma Thruster (SPT) and Thruster with Anode Layer (TAL). Over 70 SPT's have been used operationally on Soviet spacecraft since 1971¹ and a TAL D-55 has been demonstrated in space on-board a Western experimental spacecraft with its first successful firing October 23, 1998². These engines are of the 1 kW class of thrusters and have thrust levels in the 80 mN range. They have been used mostly for station keeping.

In recent years, with the advances in space power systems³, the power levels of spacecraft being manufactured have continued to rise. Spacecraft now have power levels approaching 20 kW^{4,5}. With significant power available on-board spacecraft, mission designers have begun trading the addition of high power, and relatively high thrust electric propulsion systems for launch vehicle-class reductions.⁶ To provide these in-space electric propulsion systems, NASA's Advanced Space Transportation Program initiated a high power Hall thruster program. The program focused on increasing performance and thrust for new applications such as orbit insertion, repositioning, and primary propulsion.

The program chose 10 kW as the thruster power level as it appeared to be the best choice to maximize the use of near term available spacecraft power. The other metrics for the thruster were chosen to balance fuel loading and trip time for the above applications. (Specific impulse = 2200 sec @ an efficiency > 65%).

The objective of the work reported herein was to gather preliminary data on the 10 kW for the refinement of the design point and design solution. Herein, a preliminary characterization of the first generation 10 kW laboratory Hall thruster is reported.

Apparatus

A 10 kW Hall-effect thruster, designated T-220 (Figure 1), was designed and built by TRW and Space Power Inc. under contract to NASA. The performance goals for the program can be found in Table I.

The thruster itself has a ceramic acceleration channel with an outer diameter of 220 mm and a width of 32 mm. At the bottom of this ceramic channel is the anode/gas-distributor. In the center of the ceramic channel and to the outside of the channel are toroidal electromagnet coils that generate the magnetic field. Surrounding these magnetic coils are high-permeability flux guides. The resultant magnetic field generated in

the acceleration zone by the separate inner and outer magnetic circuits is a vector combination of their independent magnetic fields.

Additionally, this first generation prototype thruster included thermocouples and potential probes for thermal data. Three thermocouples were attached to the thruster at the time of fabrication, one in the center magnet flux-guide and two on the support chassis (figure 2). Potential probes were also installed to enable accurate measurement of the resistance of the electromagnet coils for calculation of the average temperature of the coils based on the known variation of the resistance with respect to temperature. The probes were attached to the magnet wire at the bobbin used for winding.

The cathode used for this testing was based on the NASA Plasma Contactor developed for the International Space Station⁷ and was designed to operate at current levels up to 40 A with a xenon propellant flow rate of 1.5 mg/s. The cathode was positioned as shown in Figure 3.

All testing was conducted in the main volume of Vacuum Facility 5 (figure 4) at NASA GRC.⁸ This chamber is 4.6 m in diameter and 19 m in length. It is equipped with 20 – 0.8 m diameter diffusion pumps that provide approximately 100,000 l/s of Xe pumping and a gaseous helium cryogenic system which adds an additional 1.5 million l/s of Xe pumping capability.

A laboratory xenon feed system was employed for all tests. It consisted of commercially available flow controllers (with accuracy $\pm 1.0\%$ full scale), a constant volume flow calibrator, pressure transducer, and commercially available research grade xenon with purity 99.999%.

Commercially available DC power supplies were used to operate the engine. The inner magnet, outer magnet, and cathode heater supplies were all low voltage, high current supplies. The cathode keeper/ignitor supply consisted of two power supplies in parallel. A high voltage, low current ignitor supply was used to ignite the cathode and a low voltage, high current supply (protected by a blocking diode) was used to maintain cathode discharge before thruster ignition. The thruster discharge supply consisted of two 60 A, 500 V power supplies in series to give a capability of 60 A, 1000 V. An output filter consisting of a 1.0 Ω ballast resistor in series with the anode and 100 μ F capacitor between cathode and anode was used. Back-to-

back 75 volt Zener diodes were used to clamp the floating potential of the cathode to ground. A schematic of this layout can be found in Figure 5.

The thrust stand used in these tests was originally designed for a 0.5 MW Magneto-plasdynamic (MPD) thruster.⁹ The thrust stand held the thruster with its horizontal axis approximately coincident with the centerline of the vacuum facility. The stand was an inverted pendulum type design which allowed up to 25 mm of travel along the sensitive axis. An elastic restoring force was provided by the deformation of a load spring as well as the support flexures. This gave the system a natural frequency of approximately 0.25 Hz. Thrust induced deflections were measured using a linear variable differential transformer (LVDT) and recorded on a strip chart recorder. Transient motion of the thrust stand was critically damped with an electronic feedback circuit acting through an electromagnetic actuator. The damper only applied force when motion was detected, and did not affect steady-state thrust measurements.

Xenon gas for the cathode and main discharge were transferred onto the thrust stand using two separate propellant flexures. These consisted of 3 mm diameter stainless steel tubes with one end anchored to the stationary facility, and the other end attached to the moving structure of the thrust stand. Electrical current for the cathode and anode was transferred onto the stand using water cooled electrical flexures. These consisted of 6 mm diameter copper tubes supplied by a thermostatically controlled water bath. The electrical conductive spans were isolated at each end with plastic tubing. Electrical current for the cathode keeper, heater, and electromagnets were transferred onto the thrust stand with multi-conductor ribbon cables.

The thrust stand was calibrated in place and under vacuum. A mono-filament nylon line was attached to the rear of the thruster and aligned with the thrust vector. The line passed over a pulley and was drawn by weights which could be cycled on and off. The thrust stand response to the calibration weights was recorded on the strip chart, and compared directly with sessions of live thruster operation. Cycling the calibration weights revealed hysteresis on the order of 1% of the full scale value. Zero drift was also observed over period in which the thruster was fired. The amount of drift was dependent on the power

level and duration of the test. Since the drift rate was fairly consistent, for a given power level, thrust data were corrected for this error.

Procedure

Following the facility pumpdown sequence, the engine was kept at vacuum for 24 hours prior to operation to allow for outgassing of the hydroscopic components of the engine. The current limits of the discharge power supplies were set to safe limits, nominally 25 A. The Xe mass flow rate was set to desired values for both the anode and cathode. The inner and outer magnet supplies were switched on with the desired currents. After the cathode was ignited, magnets energized, and the anode was flowing Xe, the main discharge was started by ramping up the discharge voltage until breakdown occurred. The discharge voltage and power was increased to the desired value by increasing the discharge current and voltage values in a stepwise fashion.

Once the engine was running at the desired power and voltage, but prior to taking data, anode pressure was monitored as an indicator of quasi-thermal equilibrium of the thruster. Historical data have shown that thermal equilibrium of the entire thruster assembly can take as long as 10 – 20 hours of continuous operation whereas, thermal equilibrium of the anode and ceramic, which have the greatest impact on transient thruster performance, can be achieved in minutes.

Once thermal equilibrium of the anode was achieved, the engine was shut down and a thrust calibration was performed as described previously.

The engine was then restarted and testing proceeded with three series of data collection. The initial series consisted of thruster characterization of the T-220 over a range of propellant mass flow rates and discharge voltages. Magnet settings were based on ideal values predicted from modeling. The second series of tests consisted of operating the thruster at various magnet settings with constant discharge voltage and propellant mass flow rate to determine the sensitivity of the magnets on thruster efficiency. The third series of tests consisted of an extended duration firing. This firing was an attempt to gain insight into the long term operation of the engine. At the conclusion of the testing, the thruster was disassembled and

inspected to evaluate the condition of the hardware.

Results and Discussion

Characterization of the thruster was performed over a range of discharge voltages from 300-500 V and a range of discharge currents from 14.9-23 A. This corresponds to power levels from a low of 4.6 kW to a high of 10.7 kW. These data are tabulated in Table II. Specific impulses (Isp) ranged from 1644 to 2392 seconds with the desired value of 2200 seconds obtained at voltages above 400V. These data are shown in figure 6. The variation in Isp at a given voltage depicted in figure 6 was the result of different discharge currents resulting in different power levels. Furthermore, the Isp increased, for a given voltage, with increasing power over the range tested.

The range of discharge currents tested was from 14.9 to 23 A. This was accomplished with anode mass flow rates that varied from 15.7 to 22.1 mg/s of Xe. The variation of discharge current with flowrate was quasi linear as shown in figure 7. Variations in discharge current for a given flow rate were attributed to variations in the applied magnetic field strength and the discharge voltage. As can be seen this is a small effect. The effect of magnetic field strength will be discussed subsequently.

Over this range of discharge voltages the thrust varied from 278 mN to 524 mN as can be seen in figure 8. Based on the target Isp of 2200 seconds, thruster efficiency of 65%, and power level of 10 kW a thrust level of 600 mN was desired.

All the performance data reported include inefficiencies attributed to the cathode. Neither cathode position nor cathode flow rate were investigated. The cathode flow rate for all testing was a constant 1.5 mg/s. Emission currents equivalent to these discharge currents have been demonstrated with hollow cathodes of this type at flows as low as 0.4 mg/s.¹⁰ This would have a significant impact on Isp and efficiency. Additionally, the cathode-to-ground voltage during all tests was in the range of -22.1 to -27.6 V. Other Hall thrusters optimized with respect to cathode placement have exhibited cathode-to-ground voltages of approximately -10 V. This suggests that optimization of the cathode position for this thruster would also result in increased performance.

As previously mentioned, performance data were obtained after allowing the anode to reach a quasi thermal equilibrium state. The appropriate amount of time was determined based on the anode feed pressure as measured at the external Xe feed system. The actual anode pressure may have been lower if the pressure drop in the feed lines was significant. The anode pressure as well as the temperatures of the magnet flux guide and support chassis are shown in figure 9 for 40 minutes of operation. The discontinuity in feed pressure at approximately minute 10 is coincident with engine ignition. The other discontinuity over the first few minutes of thruster operation is due to the adjusting of the anode mass flow rate for the desired current. These data were taken at a discharge current of 14.9 A and a discharge voltage of 300 V. Based on these data quasi thermal equilibrium of the anode was achieved within approximately 30 to 40 minutes of operation. During this time the temperature of the magnetic flux guide and support chassis was still increasing at a rapid rate. Thermal equilibrium of the entire engine took substantially longer as will subsequently be discussed.

The effect of magnetic field strength on thruster operation has previously been demonstrated.¹¹ During this investigation the magnetic field configuration was controlled via the current to inner and outer magnets. The investigation of magnetic field strength was conducted at a discharge voltage of 500V and a discharge current of 20A. The first series was conducted by maintaining a constant 20 A in the outer magnet and varying the inner magnet current from 12 to 24 A. The second series was conducted by maintaining the inner magnet current at 20 A and varying the outer magnet current from 11 to 20 A. These data are tabulated in Tables III.

The effect of magnetic field on thruster efficiency from test series one and test series two are shown in figures 10 and 11, respectively. In both cases the efficiency peaked at approximately 55-60% at an intermediate magnet current setting. No attempt was made to completely optimize both magnets simultaneously. However, it is clear from these data that such an optimization is possible.

During the performance and magnetic field evaluations the total thruster operating time was approximately 10 hours over a period of a couple of days. In an attempt to gain insight into the long term operation of the engine a continuous

40 hour test was undertaken. During this time all the performance parameters were monitored as were several engine temperatures and the anode feed pressure. The thruster was operated at a discharge voltage of 500 V and a discharge current of 20 A. The inner magnet was set at 17 A, and the outer magnet was set at 20 A.

Figure 12 shows the temperatures of the magnetic flux guide and support chassis and the anode feed pressure as a function time. Steady-state temperatures were achieved after 3-5 hours. The engine was shut down two times during this 40 hour test, the first at approximately 8 hrs and the second at approximately 20 hrs. Both of these shut downs were initiated by the investigators. The values for the steady-state temperatures were within the design limitations for this thruster suggesting steady-state operation at higher powers is possible.

Figure 13 shows the value of discharge voltage and discharge current over the duration of this test. The voltage was essentially constant at 500V for the entire duration. The current showed a slight decline. However, the indicated anode mass flow rate remained constant. Possible explanations for this include long term drift of the anode mass flow controller or a potential gas leak between the mass flow controller and the engine.

During the extended duration testing and also during some of the earlier testing non-uniform heating of the discharge chamber was visibly observed. During normal operation the ceramic discharge chamber is below the temperature at which it would visibly glow. During these non-uniform heating events a portion of either the outer or inner discharge chamber would visibly glow a dull orange color. This seemed to have no effect on measured performance and could be effected by varying the magnetic field strength, changing the voltage, or changing the flow rate. The exact cause of this phenomenon is unclear. Possible explanations include non-uniform anode gas distribution, non-uniform magnetic field configuration, non-homogeneity in the material used to fabricate the discharge chamber, a peculiarity in the thermal design of the engine or, most probably, a combination of the above due to movement of the discharge chamber ceramic to subsequently be discussed.

Following the completion of the extended duration test, the engine was removed from the facility for visual examination. Externally the engine appeared to be as installed except for some visual wear on the outer edges of the

discharge chamber walls. Pictures of the inner and outer surfaces are shown in figures 14a, 14b. A peculiarity of the erosion evidenced on the inner discharge chamber wall was a step. This feature is approximately at the same axial location as the exit plane of the outer discharge chamber wall. This difference in length between the inner and outer discharge chamber walls is a approximately 4 mm.

A more complete physical examination revealed that the entire discharge chamber walls had moved relative to the magnetic circuit. The magnitude of the displacement was 4 mm in the positive axial direction and the entire assembly was tilted 0.5° down. This seemed to have been caused by a deficiency in the mechanical mount for this piece which then moved under the influence of gravity. It was not clear from the thruster operating data at which time this event occurred and no further erosion measurements were made. It is even possible that the motion occurred upon cooling after final shutdown. Further examination also revealed a slight gas leak in the anode propellant line. This leak was insufficient to explain the decrease in discharge current during the extended duration test. It is possible, however, that this leak became larger at operating temperature, in which case, it could explain the drop in discharge current.

Conclusions

The performance, influence of magnetic field, and thermal characteristics of a 10kW Hall thruster were measured. These data show that the performance measured (specific impulse=2392 seconds at 10kW and efficiency=59%) was close to the design point (specific impulse = 2200 seconds at 10kW and efficiency=65%). It also indicated that refinements in the cathode flow rate, anode operating point, and optimization of the magnetic field offer the possibility for improvement. The data taken over the 40 hour extended duration test indicated that the thruster design was excellent from a thermal standpoint, but requires future work in the area of mechanical durability. Erosion characteristics of the thruster were unquantifiable, qualitatively the erosion of the discharge channel seemed acceptable.

References

1. Bober, A.S. and Maslennikov. "SPT in Russia-New Achievements," Proceedings of the 24th International Electric Propulsion Conference, Sept. 1995, pp. 54-60.
2. Naval Research Laboratory, "Naval Research Laboratory Goes Operational With United States First Hall Thruster Electric Propulsion System," Press Release, October 29, 1998.
3. Bennet, G. "Aerospace Power", The Year in Review, Aerospace America, pg. 58, Dec. 1998.
4. "Hughes Unveils HS 702 Design", Aviation Week and Space Technology, p.27, Oct. 9, 1995
5. "Inside Geostationary Satellites", Launch Space, p.47, February/March, 1998
6. Oleson, S.R., Myers, R.M., "Launch Vehicle and Power Level Impacts on Electric GEO Insertion", AIAA 96-2978, July, 1996.
7. Patterson, M.J., Hamley, J.A., Sarver-Verhey, T.R., Soulas, G.C., Parkes, J.E., Ohlinger, W.L., Schaffner, M.S., and Nelson, A., "Plasma Contactor Technology for Space Station Freedom," AIAA-93-2228, June 1993.
8. Sovey, J.S., Vetrone, R.H., Grisnik, S.P., Myers, R.M., Parkes, J.E. "Test Facilities for High-Power Electric Propulsion," Journal of Propulsion and Power, Vol. 10 No.1, Jan. 1994
9. Haag, T.W., "Thrust Stand for High-Power Electric Propulsion Devices," Rev. Sci. Instrum. Vol. 62, No. 5, pp. 1186-1191, May 1991.
10. Sarver-Verhey, T.R., "Extended-Testing of Xenon Ion Thruster Hollow Cathodes," NASA CR-189227, July 1992.
11. Gavryushin, V.M., et al. "Study of the Effect of Magnetic Field Variation, Channel Geometry Change and its Walls Contamination Upon the SPT Performance," AIAA-94-2858, June 1994.

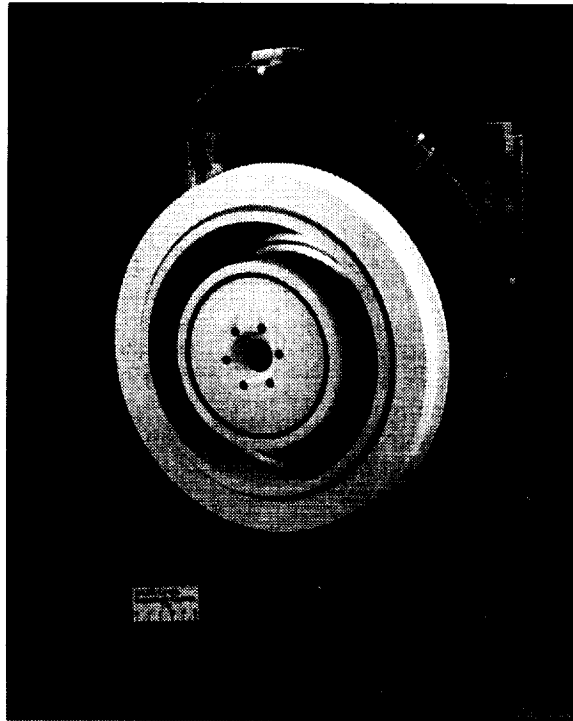


Figure 1 – T-220 Hall Effect Thruster.

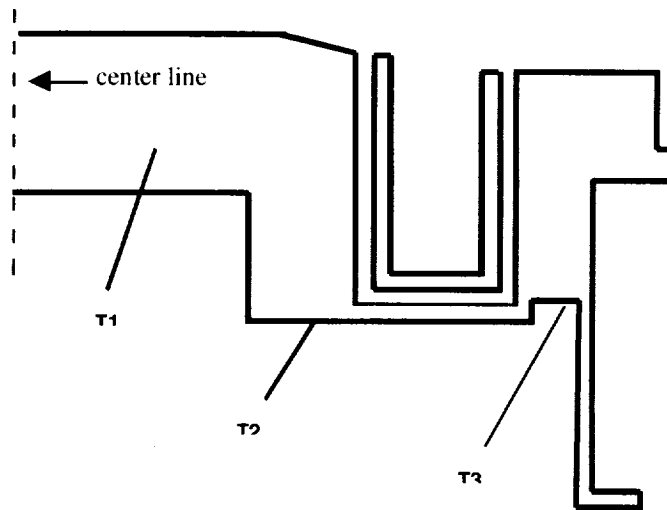


Figure 2 – Thermocouple locations.

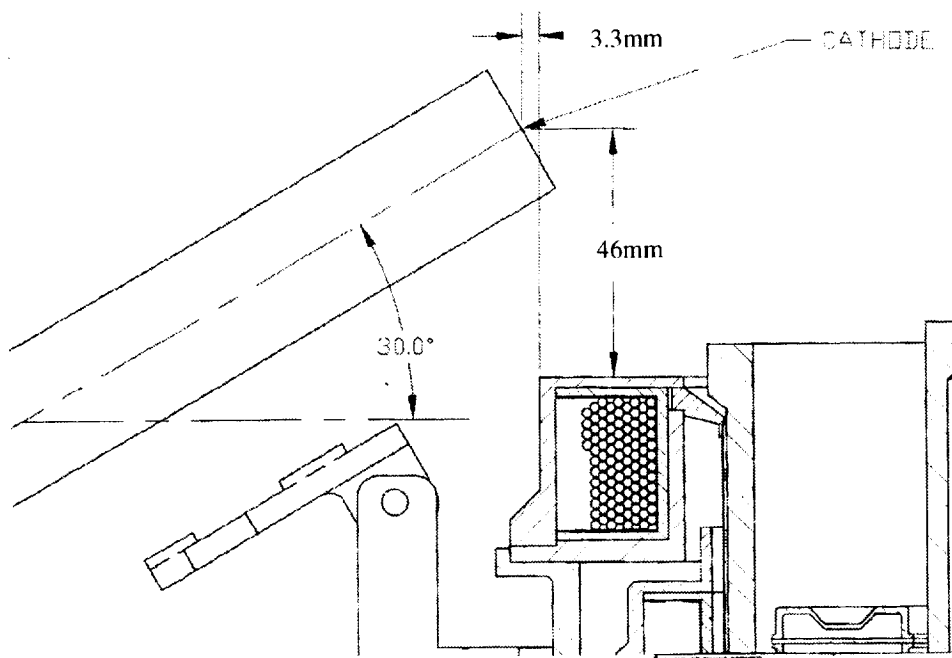


Figure 3 – Cathode Position relative to T-220 thruster.

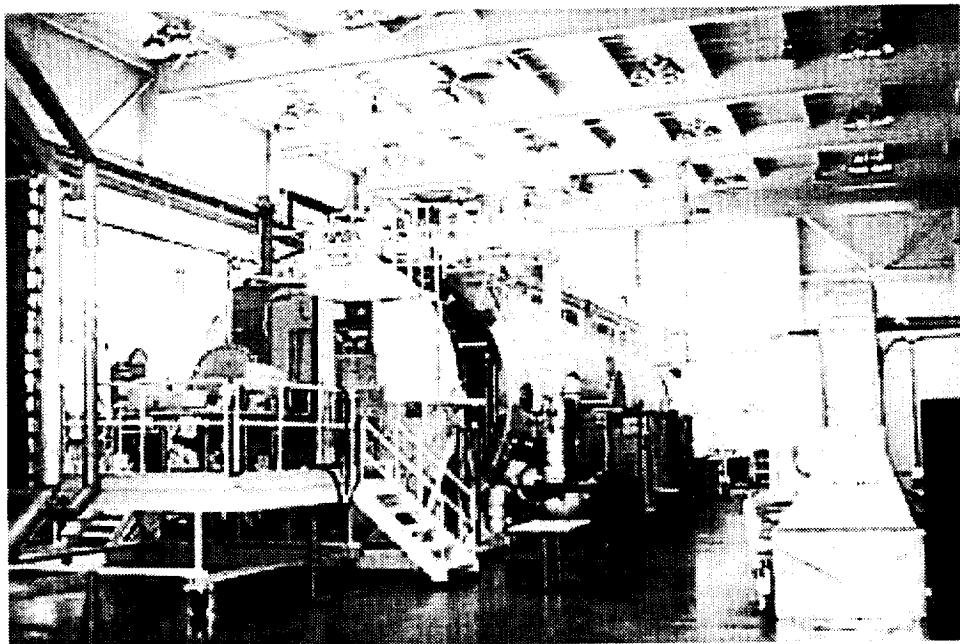


Figure 4 – Tank 5, NASA Glenn Research Center.

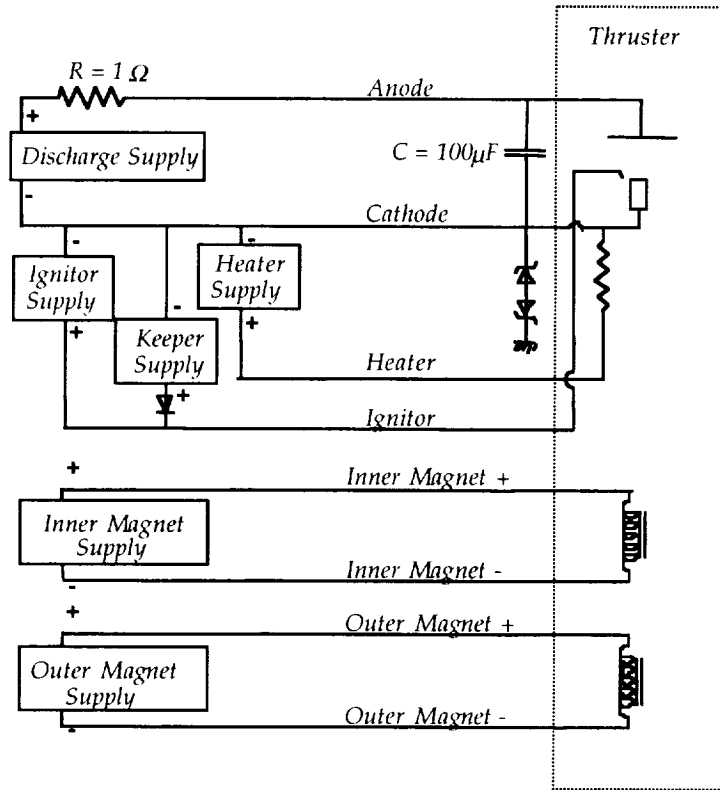


Figure 5 - Electrical schematic of T220 test setup.

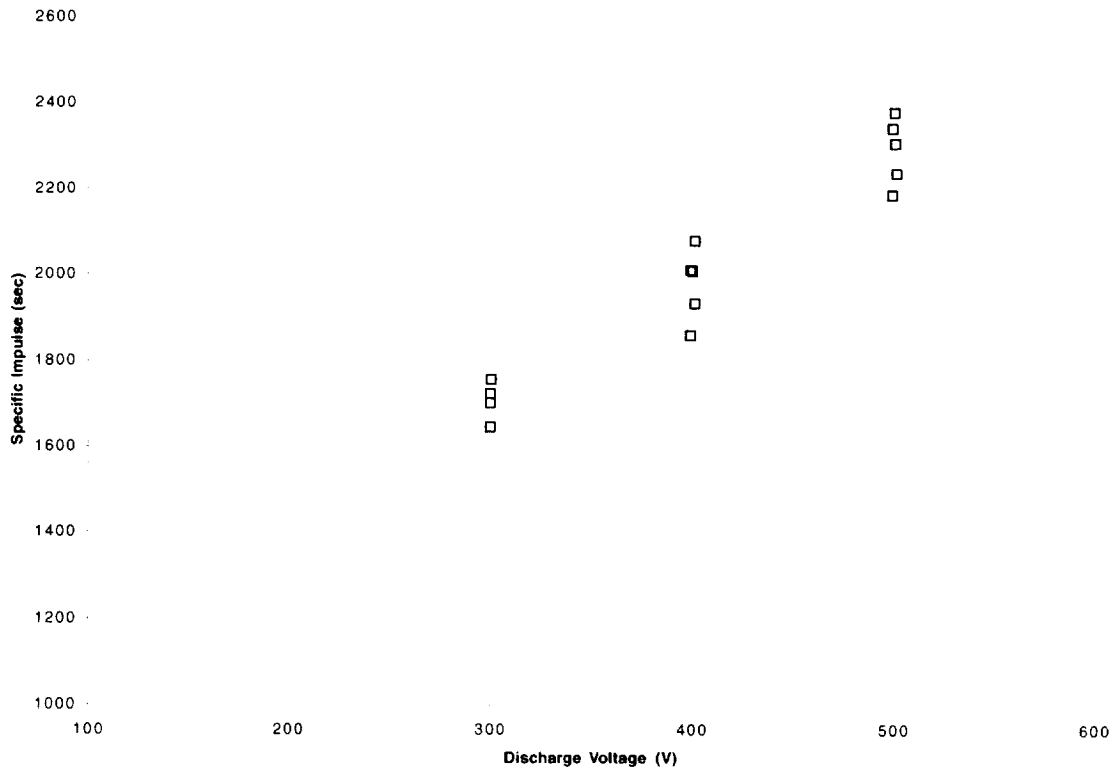


Figure 6 – Specific impulse of T220 Hall thruster as a function of discharge voltage.

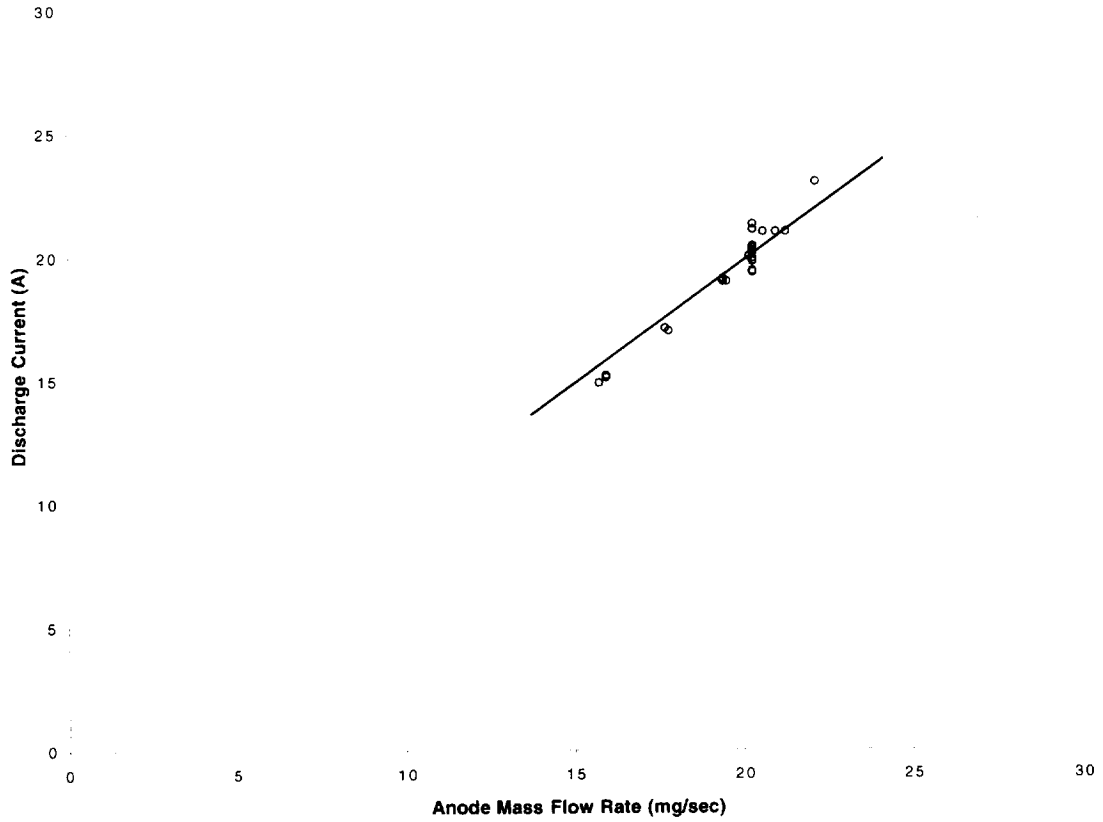


Figure 7 – Discharge current of T220 as a function of anode mass flow rate.

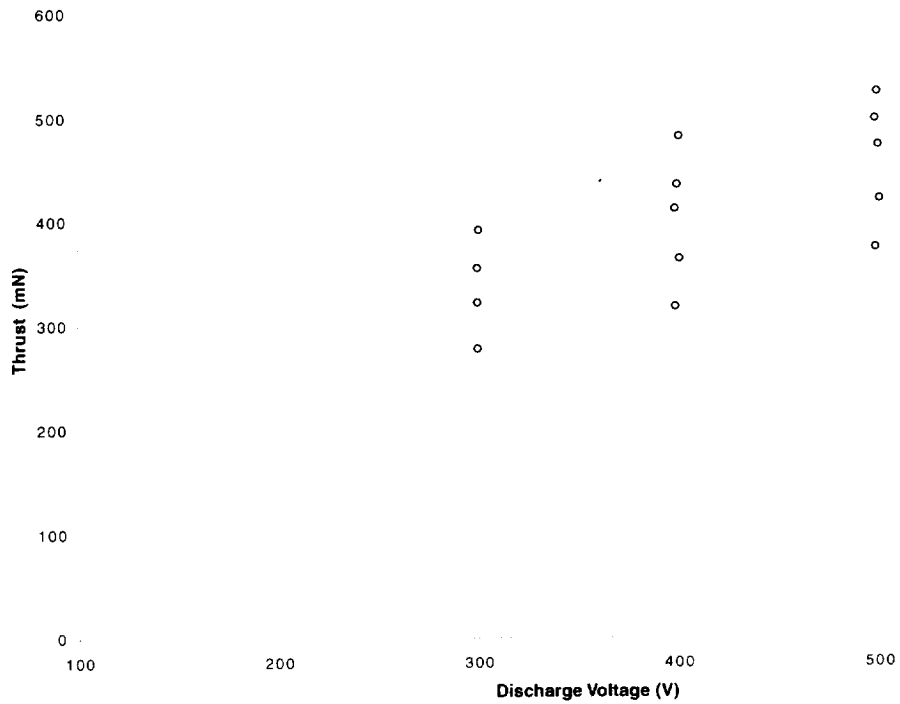


Figure 8 – Thrust of T220 Hall thruster as a function of discharge voltage.

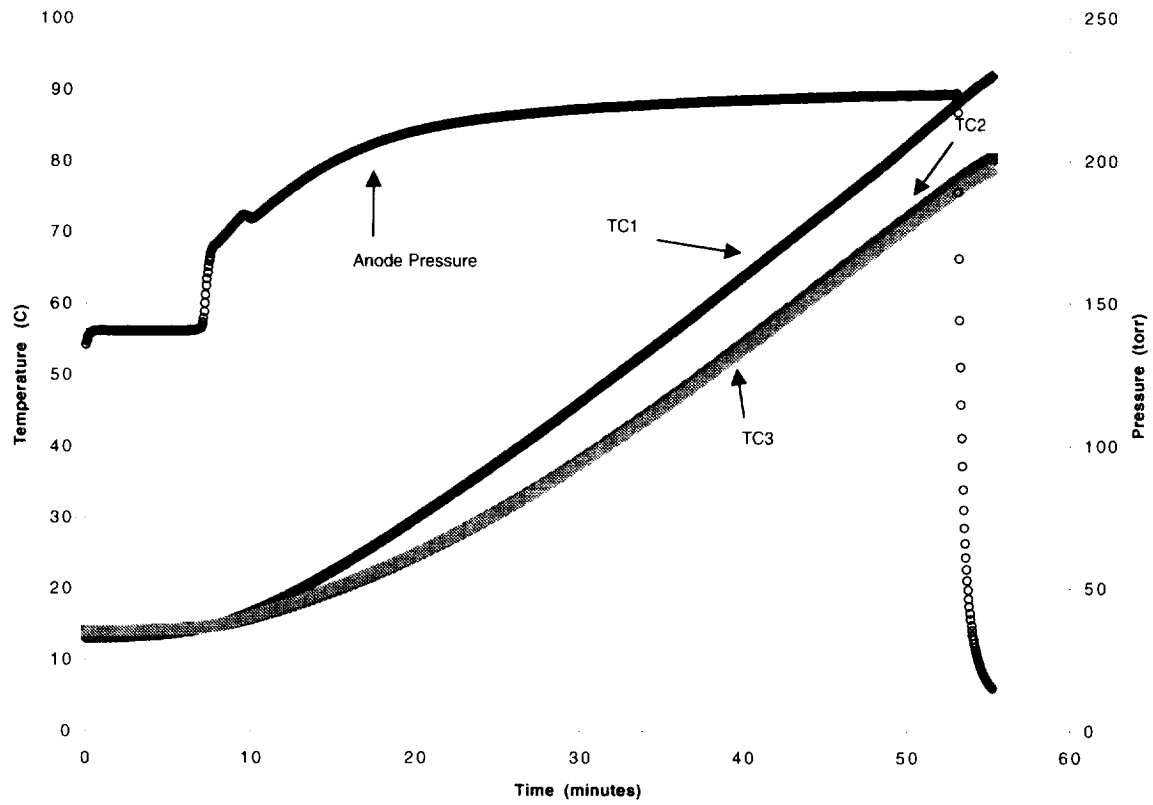


Figure 9 – Anode pressure and support structure temperature transients.

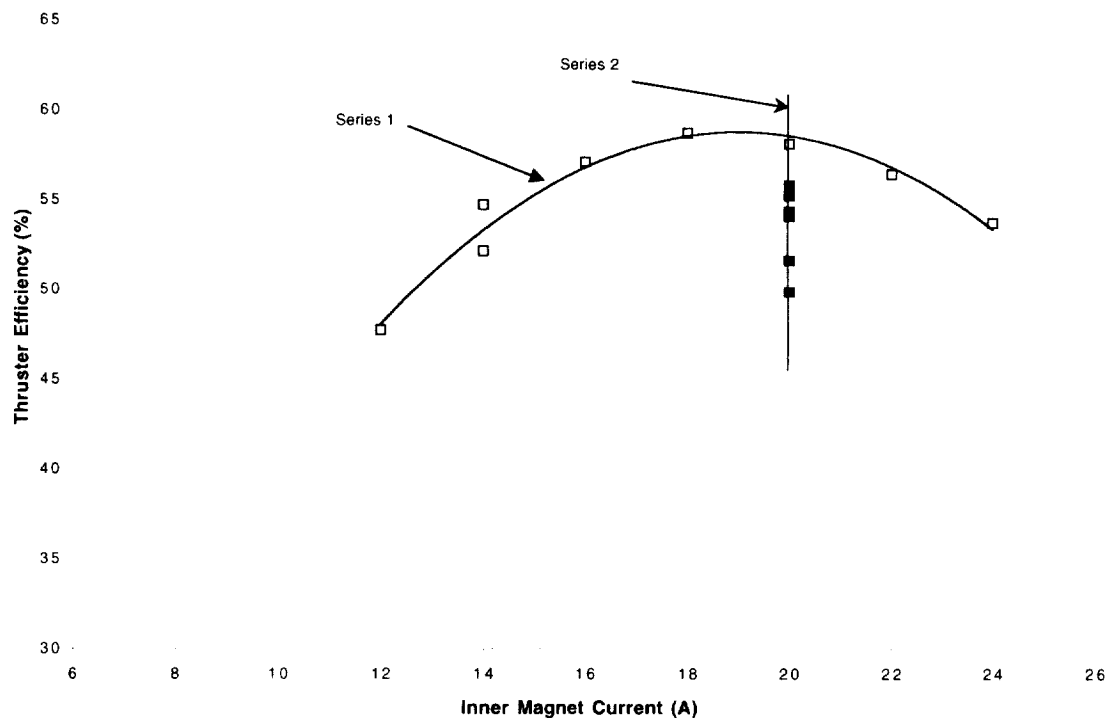


Figure 10 – Thruster efficiency as a function of inner magnet current.

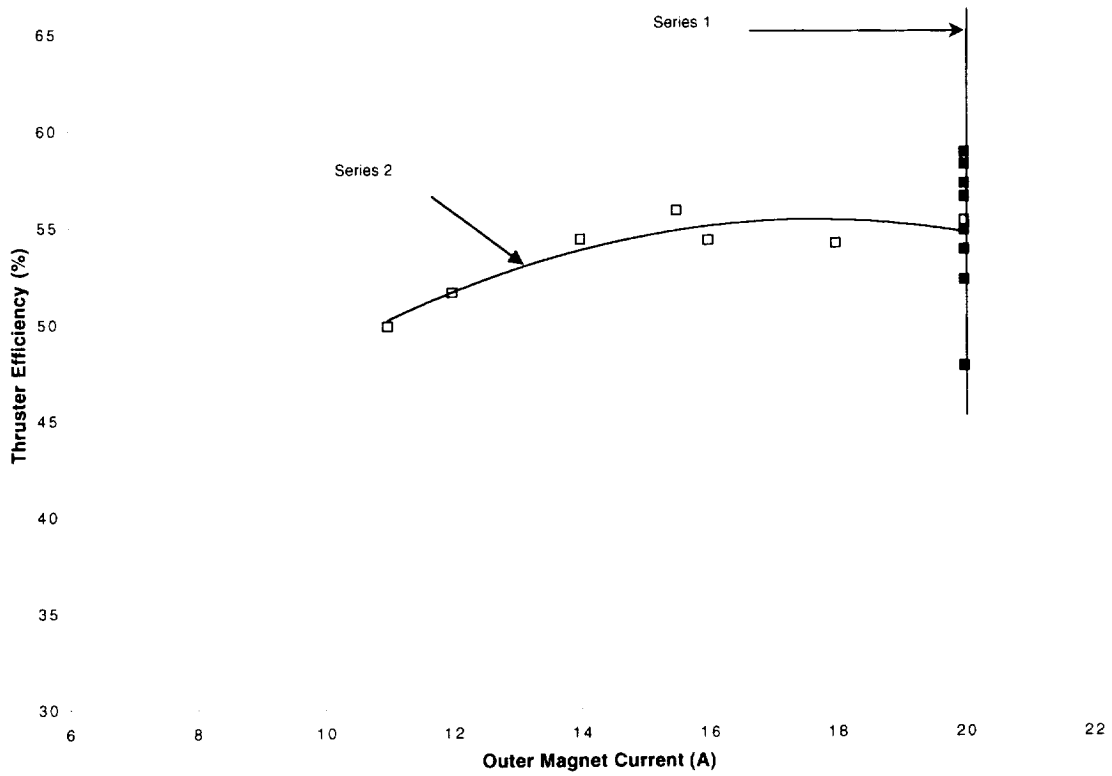


Figure 11 – Thruster efficiency as a function of outer magnet current.

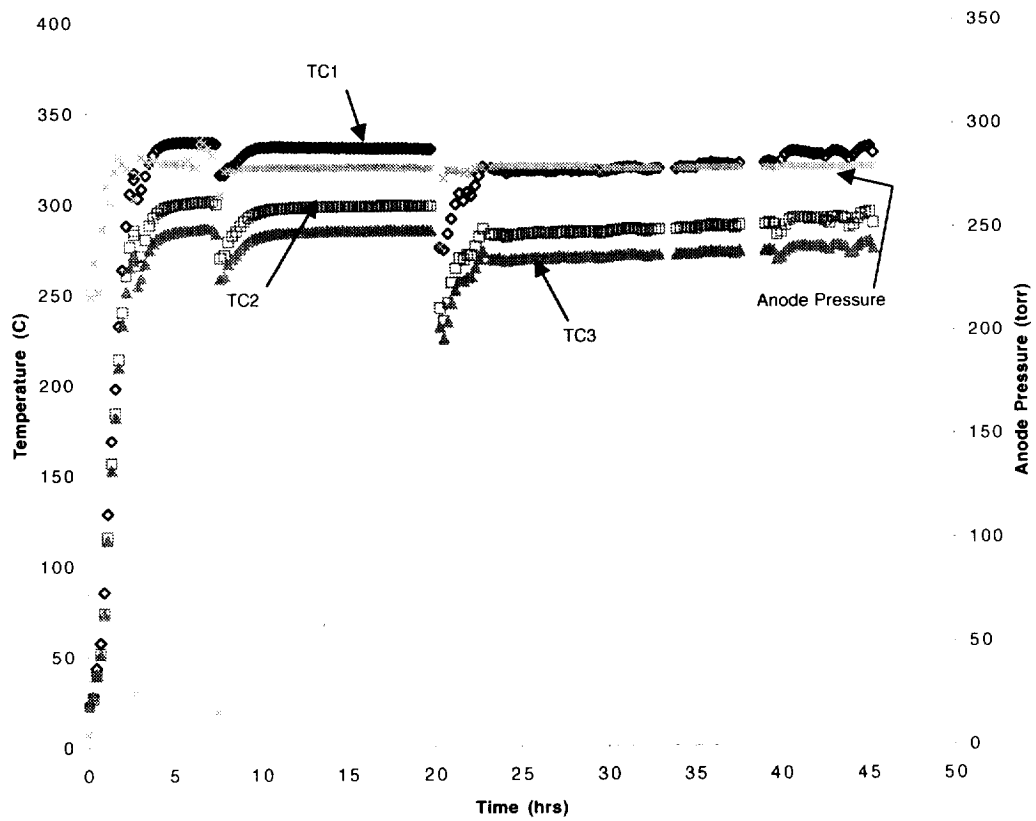


Figure 12 – Anode pressure and support structure temperature transients.

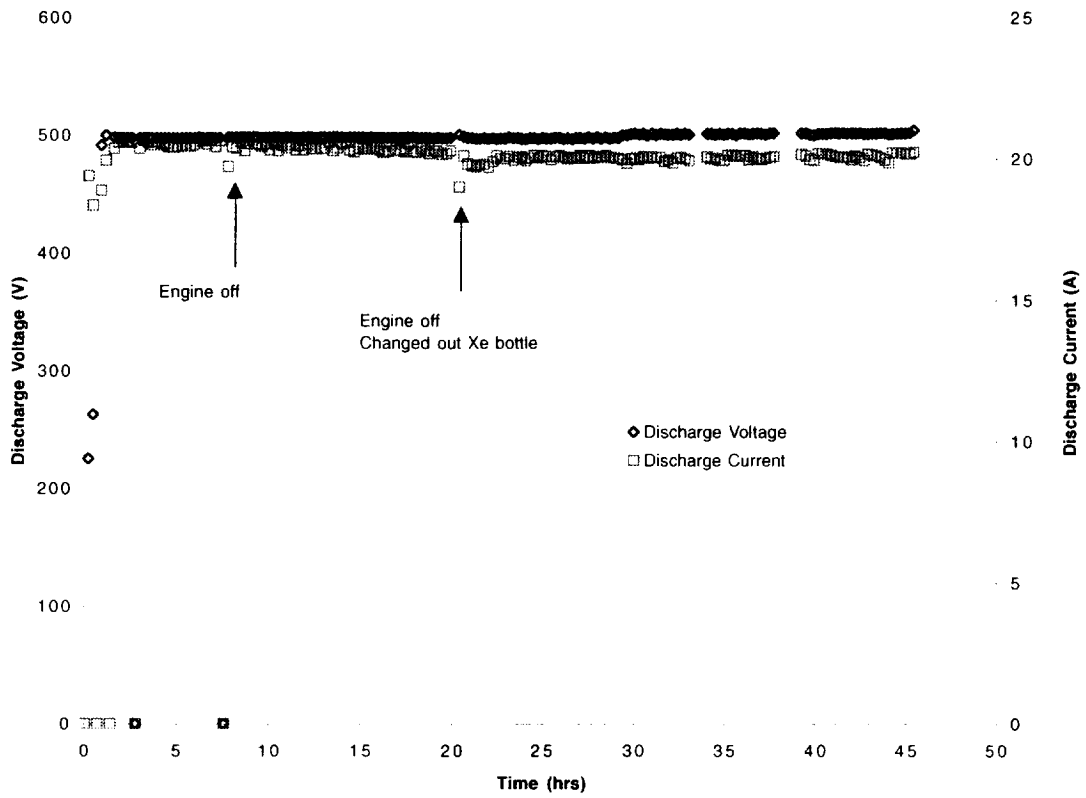
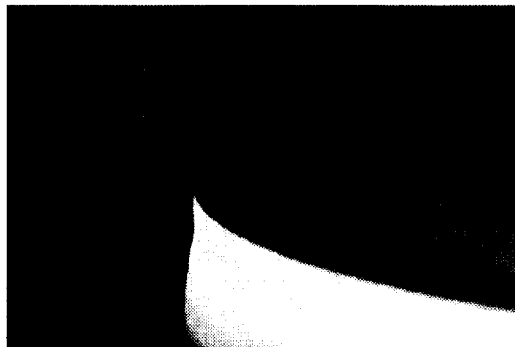


Figure 13 – Discharge voltage and discharge current for 40 hour firing.



(a) – Outer wall



(b) – Inner wall

Figure 14 – Discharge chamber wall erosion.

Metric	Goal
power (kW)	10.0
η (%)	>65%
I_{sp} (secs)	2200

Table I – Performance Targets

Test #	Time	Inner Magnet		Outer Magnet		Discharge		Mass Flow Anode	Mass Flow Cathode	Cathode-Ground	Tank pressure (calibrated on air)	
	Min.	V	A	V	A	V	A	mg/s	mg/s	V	TP1 torr	TP2 torr
PM3001	40	2.87	20	5.73	20	300	14.9	15.7	1.5	-23.3	8e-7	4e-6
PM3002	5	3.04	20	6.09	20	300	17.0	17.8	1.5	-24.7	9e-7	4e-6
PM3003	5	3.15	20	6.33	20	300	19.0	19.5	1.5	-26.3	1e-6	4e-6
PM4001	10	3.45	20	6.90	20	399	15.2	15.9	1.5	-22.4	8e-7	4e-6
PM4002	5	3.77	20	7.44	20	401	17.1	17.7	1.5	-24.6	9e-7	4e-6
PM4003	5	3.88	20	7.59	20	399	19.0	19.4	1.5	-26.6	1e-6	4e-6
PM4004	5	3.73	20	7.03	20	400	21.0	20.6	1.5	-24.1	9e-7	4e-6
PM4005	5	3.84	20	7.36	20	401	23.0	22.1	1.5	-24.3	1e-6	5e-6
PM5001	10	3.95	20	7.61	20	499	15.1	15.9	1.5	-22.1	8e-7	4e-6
PM5002	5	4.03	20	7.76	20	501	17.1	17.7	1.5	-23.5	9e-7	4e-6
PM5003	5	4.12	20	7.88	20	500	19.1	19.4	1.5	-25.6	1e-6	4e-6
PM5004	5	4.20	20	8.00	20	499	20.0	20.2	1.5	-25.7	1e-6	5e-6
PM5005	5	4.28	20	8.12	20	500	21.0	20.9	1.5	-27.6	1e-6	5e-6
PM3004	5	4.34	20	8.20	20	301	21.0	21.3	1.5	-27.5	1e-6	5e-6

Test #	TC1	TC2	TC3	Magnet Temperature		Anode pressure	thrust	Specific impulse (anode)	Efficiency (anode)	Power (anode)	Specific Impulse (total)	Efficiency (total)	Power (total)
	C	C	C	Inner C	Outer C	torr	mN	sec	%	W	sec	%	W
PM3001	84	74	73	149	166	223	278	1801	55	4470	1644	48	4642
PM3002	110	97	96	172	191	246	322	1844	57	5100	1701	51	5283
PM3003	125	110	108	186	208	270	355	1855	57	5700	1723	51	5890
PM4001	168	146	141	226	248	230	318	2034	52	6065	1859	46	6272
PM4002	217	193	185	269	286	254	364	2097	55	6857	1933	49	7081
PM4003	232	208	198	284	296	277	412	2165	58	7581	2009	52	7810
PM4004	200	170	162	264	257	285	435	2154	55	8400	2008	50	8615
PM4005	217	184	176	279	280	312	482	2219	57	9223	2079	52	9447
PM5001	234	205	194	293	298	235	374	2392	58	7535	2186	52	7766
PM5002	247	219	207	304	308	256	421	2425	59	8567	2236	52	8803
PM5003	258	230	217	316	317	278	473	2485	60	9558	2307	55	9798
PM5004	269	240	225	327	325	289	498	2516	62	9980	2342	56	10224
PM5005	278	248	233	338	334	299	524	2550	62	10500	2379	57	10748
PM3004	285	253	238	346	339	302	392	1880	57	6313	1756	51	6563

Table II – Thruster Characterization Data

Test #	Time	Inner Magnet		Outer Magnet		Discharge		Mass Flow Anode mg/s	Mass Flow Cathode mg/s	Cathode-Ground V	Tank pressure (calibrated on air)	
		V	A	V	A	V	A				TP1 torr	TP2 torr
MO2	6	5.29	24	8.27	20	505	20.3	20.3	1.5	-25.5	1E-06	5E-06
MO3	2	4.90	22	8.30	20	500	19.8	20.3	1.5	-26.2	1E-06	5E-06
MO4	1	4.46	20	8.31	20	497	19.9	20.3	1.5	-25.5	1E-06	5E-06
MO5	1	3.98	18	8.33	20	495	20.2	20.3	1.5	-24.3	1E-06	5E-06
MO6	1	3.53	16	8.35	20	495	20.4	20.3	1.5	-22.0	1E-06	5E-06
MO7	1	3.05	14	8.36	20	496	20.2	20.3	1.5	-19.9	1E-06	5E-06
MO8	1	2.61	12	8.37	20	503	21.3	20.3	1.5	-16.7	1E-06	5E-06
MO9	2	3.04	14	8.38	20	502	21.1	20.3	1.5	-18.9	1E-06	5E-06
MO10	19	4.39	20	8.21	20	501	20.4	20.3	1.5	-24.4	1E-06	5E-06
MO11	1	4.38	20	7.36	18	508	20.2	20.3	1.5	-23.0	1E-06	5E-06
MO12	1	4.40	20	6.54	16	509	19.9	20.3	1.5	-21.7	1E-06	5E-06
MO13	1	4.41	20	5.68	14	505	19.4	20.3	1.5	-20.8	1E-06	5E-06
MO14	1	4.42	20	4.82	12	501	19.4	20.3	1.5	-18.9	1E-06	5E-06
MO15	1	4.42	20	4.41	11	498	19.8	20.3	1.5	-17.7	1E-06	5E-06

Test #	TC1	TC2	TC3	Magnet Temperature		Anode pressure	thrust	Specific impulse (anode)	Efficiency (anode)	Power (anode)	Specific Impulse (total)	Efficiency (total)	Power (total)
	C	C	C	Inner C	Outer C	torr	mN	sec	%	W	sec	%	W
MO2	274	236	222	355	344	292	496	2493	59	10226	2322	54	10519
MO3	276	237	224	361	346	293	500	2513	62	9900	2340	56	10174
MO4	278	239	225	362	347	293	507	2549	64	9905	2373	58	10161
MO5	279	240	226	357	348	292	511	2569	65	9974	2392	59	10212
MO6	280	241	227	355	350	291	506	2544	63	10073	2368	57	10297
MO7	281	243	229	348	350	291	494	2483	60	10034	2312	55	10244
MO8	282	244	229	347	351	291	476	2393	52	10714	2228	48	10913
MO9	283	245	230	346	352	291	495	2488	57	10582	2317	52	10792
MO10	276	241	227	352	340	284	502	2523	61	10230	2350	55	10482
MO11	277	240	227	351	338	285	497	2498	59	10272	2326	54	10492
MO12	277	240	227	354	337	286	494	2483	59	10139	2312	54	10332
MO13	277	240	226	355	333	287	485	2438	59	9777	2270	54	9945
MO14	278	239	226	356	327	288	471	2368	56	9729	2205	52	9876
MO15	278	239	226	356	326	288	466	2343	54	9870	2181	50	10007

Table III – Magnetic Field Variation Data

REPORT DOCUMENTATION PAGE			Form Approved OMB No. 0704-0188	
Public reporting burden for this collection of information is estimated to average 1 hour per response, including the time for reviewing instructions, searching existing data sources, gathering and maintaining the data needed, and completing and reviewing the collection of information. Send comments regarding this burden estimate or any other aspect of this collection of information, including suggestions for reducing this burden, to Washington Headquarters Services, Directorate for Information Operations and Reports, 1215 Jefferson Davis Highway, Suite 1204, Arlington, VA 22202-4302, and to the Office of Management and Budget, Paperwork Reduction Project (0704-0188), Washington, DC 20503.				
1. AGENCY USE ONLY (Leave blank)	2. REPORT DATE April 1999	3. REPORT TYPE AND DATES COVERED Technical Memorandum		
4. TITLE AND SUBTITLE Preliminary Evaluation of a 10kW Hall Thruster			5. FUNDING NUMBERS WU-242-81-20-00	
6. AUTHOR(S) Robert S. Jankovsky, Chris McLean, and John McVey				
7. PERFORMING ORGANIZATION NAME(S) AND ADDRESS(ES) National Aeronautics and Space Administration John H. Glenn Research Center at Lewis Field Cleveland, Ohio 44135-3191			8. PERFORMING ORGANIZATION REPORT NUMBER E-11636	
9. SPONSORING/MONITORING AGENCY NAME(S) AND ADDRESS(ES) National Aeronautics and Space Administration Washington, DC 20546-0001			10. SPONSORING/MONITORING AGENCY REPORT NUMBER NASA TM-1999-209075 AIAA-99-0456	
11. SUPPLEMENTARY NOTES Prepared for the 37th Aerospace Sciences Meeting & Exhibit sponsored by the American Institute of Aeronautics and Astronautics, Reno, Nevada, January 11-14, 1999. Robert S. Jankovsky, NASA Glenn Research Center; Chris McLean and John McVey, Space Power, Inc., San Jose, California 95134. Responsible person, Robert S. Jankovsky, organization code 5430, (216) 977-7515.				
12a. DISTRIBUTION/AVAILABILITY STATEMENT Unclassified - Unlimited Subject Categories: 18 and 20 This publication is available from the NASA Center for AeroSpace Information, (301) 621-0390.			12b. DISTRIBUTION CODE	
13. ABSTRACT (Maximum 200 words) A 10 kW Hall thruster was characterized over a range of discharge voltages from 300-500 V and a range of discharge currents from 15-23 A. This corresponds to power levels from a low of 4.6 kW to a high of 10.7 kW. Over this range of discharge powers, thrust varied from 278 mN to 524 mN, specific impulse ranged from 1644 to 2392 seconds, and efficiency peaked at approximately 59%. A continuous 40 hour test was also undertaken in an attempt to gain insight with regard to long term operation of the engine. For this portion of the testing the thruster was operated at a discharge voltage of 500 V and a discharge current of 20 A. Steady-state temperatures were achieved after 3-5 hrs and very little variation in performance was detected.				
14. SUBJECT TERMS Hall thruster; Electric propulsion			15. NUMBER OF PAGES 20	
			16. PRICE CODE A03	
17. SECURITY CLASSIFICATION OF REPORT Unclassified	18. SECURITY CLASSIFICATION OF THIS PAGE Unclassified	19. SECURITY CLASSIFICATION OF ABSTRACT Unclassified	20. LIMITATION OF ABSTRACT	

